[Fe₄] and [Fe₆] Hydride Clusters Supported by Phosphines: Synthesis, Characterization, and Application in N₂ Reduction

Ryoichi Araake,[†] Kazuki Sakadani,[†] Mizuki Tada,[†,§] Yoichi Sakai,[¶] and Yasuhiro Ohki[*,†,‡]*

[†]Department of Chemistry, Graduate School of Science, and [§]Research Center for Materials Science and Integrated Research Consortium on Chemical Sciences, Nagoya University, Furo-cho, Chikusa-ku, Nagoya 464-8602, Japan

[¶]Department of Chemistry, Daido University, Takiharu-cho, Minami-ku, Nagoya 457-8530, Japan

[‡]PRESTO, Japan Science and Technology Agency (JST), Honcho, Kawaguchi, Saitama 332-0012, Japan

ABSTRACT: Multiple iron atoms bridged by hydrides is a common structural feature of the active species that have been postulated in the biological and industrial reduction of N_2. In this study, the reactions of an Fe(II) amide complex with pinacolborane in the presence/absence of phosphines afforded a series of hydride-supported [Fe₄] and [Fe₆] clusters $Fe_4(\mu\text{-}H)_4(\mu_3\text{-}H)_2\{N(SiMe_3)_2\}_2(PR_3)_4$ [PR_3 = PMe_3 (**2a**), PMe_2Ph (**2b**), PEt_3 (**2c**)], $Fe_6(\mu\text{-}H)_{10}(\mu_3\text{-}H)_2(PMe_3)_{10}$ (**3**), and $(\eta^6\text{-}C_7H_8)Fe_4(\mu\text{-}H)_2\{\mu\text{-}N(SiMe_3)_2\}_2\{N(SiMe_3)_2\}_2$ (**4**), which were characterized crystallographically and spectroscopically. Under ambient conditions, these clusters catalyzed the silylation of N_2 to furnish up to 160±13 equiv. of $N(SiMe_3)_3$ per **2c** (40 equiv. per Fe atom) and 183±18 equiv. per **3** (31 equiv. per Fe atom). With regard to the generation of the reactive species, dissociation of phosphine and hydride ligands from the [Fe₄] and [Fe₆] clusters was indicated, based on the results of the mass spectrometric analysis on the [Fe₆] cluster, as well as the formation of a diphenylsilane adduct of the [Fe₄] cluster.

Introduction

Iron-hydride species, particularly those containing multiple iron and hydrogen atoms, are important intermediates in the biological and industrial reduction of N_2. The biological reduction of N_2 is mediated by the active site of the nitrogenase enzyme (FeMo-cofactor), which features a [MoFe₇S₉C] core supported by an *R*-homocitrate, as well as one cysteine and one histidine residue.[1,2] It has been proposed that some of the inner iron atoms of the FeMo-cofactor participate during the activation of N_2.[3] This notion was supported by a protein crystal structure of one of the CO-inhibited forms revealing a Fe-CO-Fe moiety, which resulted from the capture of a CO molecule by two inner iron atoms of the FeMo-cofactor.[4] The importance of iron hydrides in the biological fixation of N_2 was furthermore supported by detailed biochemical and spectroscopic analyses on the FeMo-cofactor in the active form, which suggested the presence of Fe-H-Fe hydride moieties and a release of H_2 from them during the activation of N_2.[3,5,6] In the Haber-Bosch process, which is used for the industrial production of ammonia, metallic iron is treated with a mixture of N_2 and H_2, and iron-hydride species need to be formed prior to the formation of N-H bonds.[7-10] Even though the reaction conditions and the reaction pathways are thus different in biological and industrial processes, multiple iron atoms and bridging hydrides represent two common features.

In relation to the intermediacy of bridging hydrides in the fixation of N_2, some dinuclear/trinuclear hydride complexes have been employed for the activation of N_2. A seminal example is $[NPN]Ta(\mu\text{-}H)_4Ta[NPN]$ ($[NPN]$ = $C_6H_5P(CH_2SiMe_2\text{-}NC_6H_5)_2$), which activates N_2 through the reductive elimination of H_2.[11] More advances with early transition metals include dianionic $Nb(\mu\text{-}H)_4Nb$ and neutral $Ti_3(\mu\text{-}H)_6(\mu_3\text{-}H)$ complexes,[12,13] which are prone to cleave the triple bond of N_2 via liberation of H_2. For the [Ti₃] hydride cluster, the formation of an N-H bond has been observed.[13] Some $Fe(\mu\text{-}H)_2Fe$ complexes supported by β-diketiminates release H_2 and accommodate N_2 under irradiation from a high-pressure mercury lamp,[14] and a dianionic $Co(\mu\text{-}H)_2Co$ analogue incorporates N_2 even without irradiation.[15] A $Fe(\mu\text{-}H)_2Fe$ complex supported by a hexadentate phosphine-silyl ligand strongly binds N_2 in its mixed-valent Fe(II)Fe(I) state.[16] In this study, we synthesized well-defined molecular clusters consisting of multiple iron atoms and bridging hydrides. The key step in the synthetic protocol used herein is the reaction between an $Fe\text{-}N(SiMe_3)_2$ moiety and pinacolborane (HBpin), which leads to the generation of Fe-H species under concomitant liberation of $(Me_3Si)_2N\text{-}Bpin$. Similar reactions have been observed in our previous studies for the generation of $(\eta^5\text{-}C_5Me_5)Fe$-hydride species[17] and cobalt hydride clusters.[18] Herein, we report the synthesis and characterization of phosphine-supported [Fe₄] and [Fe₆] clusters with multiple bridging hydrides. These clusters can serve as catalyst precursors in the reductive conversion of N_2 into $N(SiMe_3)_3$. These Fe clusters were also employed in the attempted synthesis of NH_3.
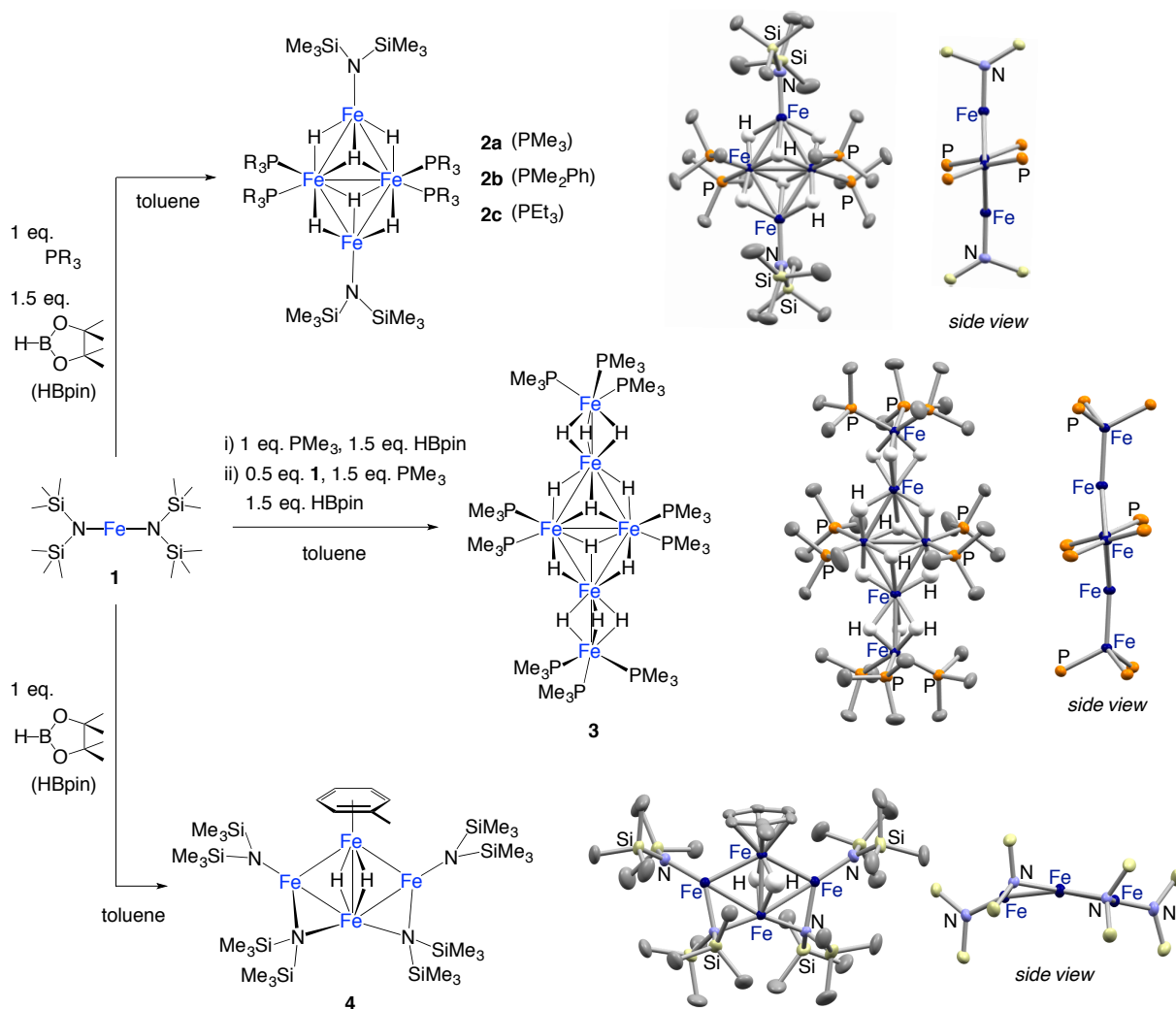
Results and Discussion

Synthesis and Structures of the [Fe₄] and [Fe₆] Hydride Clusters. The reaction of the Fe(II) amide complex $Fe\{N(SiMe_3)_2\}_2$ (**1**)[19] with 1 equiv. of phosphine (PR_3) and 1.5

equiv. of HBpin resulted in the formation of black solutions, from which the [Fe4] hydride clusters Fe$_4$(μ-H)$_4$(μ_3-H)$_2$\{N(SiMe$_3$)$_2$\}$_2$(PR$_3$)$_4$ (**2a**: R = Me, **2b**: R$_3$ = Me$_2$Ph, **2c**: R = Et) precipitated as black crystals in 11-18% yield (Scheme 1). Crystals of the [Fe6] cluster Fe$_6$(μ-H)$_{10}$(μ_3-H)$_2$(PMe$_3$)$_{10}$ (**3**) precipitated in 14% yield from the sequential treatment of *in-situ*-generated **2a** with **1**, PMe$_3$, and HBpin.[20] Based on their chemical formulae, an average Fe(II) oxidation state should be applied to **2a-c** and **3**. The synthetic routes to these clusters thus proceeded under retention of the oxidation state, via replacement of bulky –N(SiMe$_3$)$_2$ ligands with hydrides to generate low-coordinate Fe-hydride species in the presence or absence of phosphines, followed by their assembly through hydride bridges and further accommodation of phosphines. The low yields of the crystalline clusters **2a-c** and **3** indicate the formation of byproducts, one of which was identified as the toluene-bound [Fe4] cluster (η^6-C$_7$H$_8$)Fe$_4$(μ-H)$_2$\{μ-N(SiMe$_3$)$_2$\}$_2$\{N(SiMe$_3$)$_2$\}$_2$ (**4**), which was isolated in crystalline form in 12% yield when the reaction of **1** with 1 equiv. of HBpin was carried out in the absence of phosphines in toluene at 0 °C. The chemical formul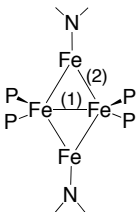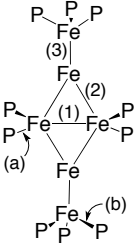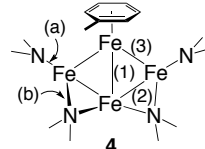a of **4** leads to an average oxidation state of Fe(+1.5). The same compound was simultaneously synthesized by Jacobi von Wangelin *et al.* from the reaction of **1** with ^{i}Bu$_2$AlH in toluene.[21] However, they did not detect bridging hydrides, as a detailed spectroscopic assignment was beyond the scope of their primary work. The different assignment of the number of hydrides in **4** highlights the difficulty to identify hydrides in paramagnetic clusters. From an analogous reaction in hexane at room temperature, a small amount of crystals, containing the hexagram-shaped [Fe7] cluster Fe$_7$(μ_3-H)$_6$\{μ-N(SiMe$_3$)$_2$\}$_6$ was obtained (Figure S17). However, the isolation of this complex was hampered by the fact that it co-crystallized with Fe$_6$(μ_3-H)$_4$(μ-H)$_2$\{μ-N(SiMe$_3$)$_2$\}$_4$\{N(SiMe$_3$)$_2$\}$_2$ as the major species, which is the corresponding analogue containing one less Fe atom. A single-crystal X-ray diffraction analysis revealed a compositional disorder of [Fe6] and [Fe7] clusters. This result stands in contrast to the cobalt congener Co$_7$(μ_3-H)$_6$\{μ-N(SiMe$_3$)$_2$\}$_6$,[18] which appears as a single component. It should be noted that compositional disorder of the [Fe6] and [Fe7] clusters was also reported for crystals obtained from the reaction of **1** with ^{i}Bu$_2$AlH in hexane.[21]

Scheme 1. Synthesis and Structures of Fe-Hydride Clusters 2a-c, 3, and 4.[a]

[a] In the molecular structures (atomic displacement parameters set at 50% probability), only selected atoms are labeled, and hydrogen atoms except for the hydrides are omitted for clarity. In the side views, carbon and hydrogen atoms are omitted for clarity.

Table 1. Selected Inter-Atomic Distances (Å) in [Fe$_4$] and [Fe$_6$] Clusters.

		2a (PMe$_3$)	2b (PMe$_2$Ph)	2c (PEt$_3$)
	Fe-Fe(1)	2.6452(4)	2.6555(5)	2.6790(5)
	Fe-Fe(2)	2.5133(5)	2.5264(5)	2.5318(4)
		2.5173(4)	2.5283(5)	2.5436(5)
	Fe-P	2.1596(6)	2.1652(7)	2.1836(9)
		2.1608(6)	2.1725(7)	2.1862(6)
	Fe-N	1.9410(13)	1.942(2)	1.9497(18)

3

Fe-Fe(1)	2.6226(5)	
Fe-Fe(2)	2.5659(5), 2.5703(5)	
Fe-Fe(3)	2.4344(5)	
Fe-P(a)	2.1510(6), 2.1523(6)	
Fe-P(b)	2.1558(6), 2.1584(6), 2.1596(7)	

4

Fe-Fe(1)	2.4895(14)
Fe-Fe(2)	2.6317(13), 2.6481(10)
Fe-Fe(3)	2.5603(12), 2.5989(10)
Fe-N(a)	1.948(4), 1.949(3)
Fe-N(b)	2.066(4)-2.082(4)
Fe-C$_{toluene}$	2.108(5)-2.132(6)

The molecular structures of the [Fe$_4$] and [Fe$_6$] hydride clusters shown in Scheme 1 (*cf.* Figures S14-S15) reveal that the Fe atoms in these clusters adopt a crystallographically coplanar or virtually coplanar arrangement, while the hydrides serve as doubly or triply bridging ligands. As listed in Table 1, the Fe-Fe distances vary depending on the number and the bridging mode of the hydride ligands, even though all Fe-Fe distances fall in the range of Fe-Fe bonds. The μ-H ligands afford shorter Fe-Fe distances relative to the μ$_3$-H ligands, and for instance, the shortest Fe-Fe distance in 3 was observed in the Fe(μ-H)$_3$Fe moiety (2.4344(5) Å), while the longest Fe-Fe distance in 3 (2.6226(5) Å) involves two μ$_3$-H ligands. In the phosphine-supported [Fe$_4$] clusters 2a-c, the Fe-Fe bonds involving two μ$_3$-H ligands (2.6452(4)-2.6790(5) Å) were also longer than those involving one μ-H and one μ$_3$-H ligands (2.5133(5)-2.5436(5) Å). Within the [Fe$_4$] core of 4, two μ-H ligands bridge the diagonal Fe-Fe bond, which is shorter (2.4895(14) Å) than other Fe-Fe bonds without hydride bridges (2.5603(12)-2.6481(10) Å). Given the Fe-P and Fe-N(SiMe$_3$)$_2$ bond lengths in clusters 2a-c and 3 (Fe-P: 2.1510(6)-2.1862(6) Å; Fe-N: 1.9410(13)-1.9497(18) Å), these fall in the range of typical six-coordinate Fe(II)-PR$_3$ (2.1657(12)-2.379(2) Å)[22,23] and four-coordinate Fe(II)-N(SiMe$_3$)$_2$ (1.934(2)-2.009(2) Å)[24,25] complexes, and are consistent with an average Fe(II) oxidation state for these clusters. The relatively short Fe-P and Fe-N distances can be rationalized in terms of the relatively low steric hindrance around the Fe atoms imposed by the coordination of multiple hydrides. The Fe-Fe and Fe-P distances in 2a-c follow the order 2a < 2b < 2c, reflecting the steric congestion arising from the phosphine ligands. Even though the average oxidation state of Fe(+1.5) is relatively low in cluster 4, the assignment of the oxidation states of the Fe centers was not trivial. The terminal Fe-N(SiMe$_3$)$_2$ distances (1.948(4)/1.949(3) Å) are comparable to those in 2a-c and 3, and the Fe-{μ-N(SiMe$_3$)$_2$} distances (2.066(4)-2.082(4) Å) fall in the

longer regions of previously reported Fe(II)-{μ-N(SiMe$_3$)$_2$} distances (1.979(2)-2.099(3) Å).[17,26] The (η^6-toluene)Fe moiety in 4 exhibits Fe-C distances (2.108(5)-2.132(6) Å) in the range of typical Fe-C(η^6-arene) distances reported for complexes of Fe(0), Fe(I), Fe(II), and Fe(IV).
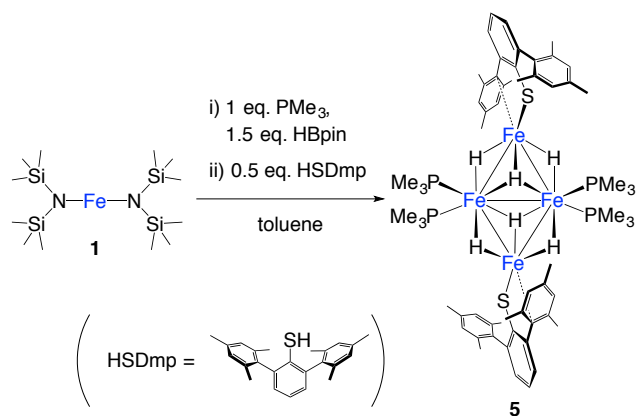
Spectroscopic characterization of the [Fe$_4$] and [Fe$_6$] hydride clusters. Clusters 2a-c, 3, and 4 are paramagnetic and their ^{1}H NMR spectra in C$_6$D$_6$ exhibited broad signals for phosphines and amides in the range of *ca.* +50 to –85 ppm (Table 2 and Figures S1-5). Solution magnetic moments (μ$_{eff}$) for 2a-c (8.3(1)-11.2(1) μ$_B$), 3 (6.8(3) μ$_B$), and 4 (5.7(1) μ$_B$) at 298 K indicate interactions across multiple d-orbitals via Fe-Fe bonds, leading to the formation of multiple orbitals in a narrow energy range to store unpaired d-electrons. Although hydride signals were not observed in the ^{1}H NMR spectra, the assigned formula of [Fe$_6$] cluster 3 was supported by its electro-spray ionization mass spectrum (ESI-MS) in THF (Figure S8). The signal of the 1e-oxidized form [3]$^+$ appeared at m/z = 1108.0, and the isotope pattern of this peak was consistent with that calculated from the structure of 3 featuring twelve hydrides. Furthermore, the ESI-MS signal of deuterated 3, which was prepared from the reaction of 1, PMe$_3$, and DBpin in toluene, was shifted on average by twelve units (m/z = 1120.1). In contrast to the successful ESI-MS observation of [3]$^+$, the corresponding ESI-MS signals for [Fe$_4$] clusters 2a-c and 4 were not observed, probably due to unsuccessful oxidation or reduction in the spectrometer. Therefore, cyclic voltammograms (CVs) of clusters 2b, 3, and 4 were measured. The [Fe$_6$] cluster 3 exhibited one oxidation and one reduction at $E_{1/2}$ = –1.76 V and –2.96 V (vs Fc/Fc$^+$; Fc = (η^5-C$_5$H$_5$)$_2$Fe), whereby the former occurs at only slightly more positive potential than the rest potential (–1.81 V) (Figure S11). Conversely, the redox potentials of 2b ($E_{1/2}$ = –0.58 V and –2.11 V) are substantially different from the rest potential (–1.37 V) (Figure S10). The large separation of 2b is consistent with the unsuccessful ESI-MS measurements, even though the relatively large potential gap should not be the sole reason for the presence/absence of an ESI-MS signal. As all the amide-supported clusters in this study (2a-c, 4, and 6) are ESI-MS inactive, the presence of the amide ligands possibly hampers the measurements. For example, the steric congestion arising from the bulky –N(SiMe$_3$)$_2$ ligands could lead to an enhanced electric resistance, that is consistent with the relatively large separation observed for the anodic/cathodic peaks of 2b.

Table 2. ^{1}H NMR Chemical Shifts (ppm) of [Fe$_4$] and [Fe$_6$] Clusters in C$_6$D$_6$.

Cluster	N(Si*Me*$_3$)$_2$	PR$_3$ and other signals
2a	47.3	–75.1 (PC*H*$_3$)
2b	50.7	–84.7 (PC*H*$_3$), –79.0 (*o*- or *m*-Ph)
		–13.1 (*o*- or *m*-Ph), –7.1 (*p*-Ph)
2c	49.8	–84.6 (PC*H*$_2$CH$_3$)
		–57.7 (PCH$_2$C*H*$_3$),
3		–71.5 (P*Me*$_3$ x 4), 42.0 (P*Me*$_3$ x 6)
4	–5.3	–23.6 (*o*- or *m*-H), –20.7 (C$_6$H$_5$C*H*$_3$)
	–1.9	–12.5 (*p*-H), 53.4 (*o*- or *m*-H)

For the ESI-MS identification of the number of hydrides present in the phosphine-supported [Fe$_4$] clusters, a thiolate-substituted analogue of 2a, Fe$_4$(μ-H)$_4$(μ$_3$-H)$_2$(SDmp)$_2$(PMe$_3$)$_4$ (5; Dmp = 2,6-

Scheme 2. Synthesis of a Thiolate-Supportd [Fe$_4$] Hydride Cluster 5.

(mesityl)$_2$C$_6$H$_3$), was synthesized in 11% yield by treatment of *in-situ*-generated **2a** with HSDmp (Scheme 2). The ESI-MS spectrum of **5** in THF exhibited a signal for [**5**]$^+$ at *m/z* = 1224.3 (Figure S9), which shifted by six units for the deuterium-labeled analogue (*m/z* = 1230.1). In accordance with the proposed dependence of the appearance of ESI-MS signals on the gap between the rest potential and the redox processes, the cyclic voltammogram of **5** exhibited an oxidation and a reduction process at $E_{1/2}$ = –1.07 V and –2.54 V (Figure S13), respectively, and the separation (0.43 V) between the former and the rest potential (–1.50 V) is intermediate to those of **3** (0.05 V) and **2b** (0.79 V). The molecular structure of **5** revealed that the [Fe$_4$(μ-H)$_4$(μ$_3$-H)$_2$(PMe$_3$)$_4$] core is almost identical to that of **2a**, and this similarity is reflected in the bond distances for *e.g.* the diagonal Fe1-Fe1* bond (**5**: 2.6324(4) Å; **2a**: 2.6452(4) Å), the Fe1-Fe2 bond at the edges of the rhombus (**5**: 2.4953(4) and 2.4977(4) Å; **2a**: 2.5133(5) and 2.5173(4) Å), and the Fe-PMe$_3$ bonds (**5**: 2.1645(9) and 2.1715(6) Å; **2a**: 2.1596(6) and 2.1608(6) Å) (Figure S16). In contrast to the terminal coordination of the –N(SiMe$_3$)$_2$ ligands in **2a**, the SDmp ligand in **5** probably uses one of the mesityl rings in addition to the sulfur atom for the interactions with Fe, leading to a coordination geometry that is different from that of **2a**. Although the Fe···C(mesityl) distance (2.7800(19) Å) is significantly longer than those in typical Fe-arene complexes, relevant weak Fe-mesityl interactions have been observed in Fe-SDmp complexes (Fe-C: 2.389(2)-2.694(2) Å).[27-31] The postulated weak Fe-mesityl interaction in **5** possibly contributes to the appearance of two sets of mesityl signals in the ^{1}H NMR spectrum (Figure S6). One of the sets appeared as broad and shifted signals, while the other was observed as relatively sharp signals with chemical shifts that are typical for mesityl groups. The significant broadening and shift of one of these sets of signals indicates a close proximity of the associated mesityl group to the Fe center, which would induce a strong paramagnetic effect, while the other mesityl group should be sufficiently separated from Fe to limit the magnetic influence on the NMR spectrum.

The presence of hydrides in **2a-c**, **3**, and **5** was further indicated by the infrared (IR) spectra (Figures 1 and S18-21). For instance, a broad Fe-H band was observed for **2b** at 1524 cm^{-1}, which shifted to 1108 cm^{-1} for the deuterated analogue. Similarly, the difference spectrum between **3** and deuterated **3** exhibited broad Fe-H bands at 1670, 1610, and 1498 cm^{-1}, which shifted to 1233, 1190, and 979 cm^{-1} upon deuteration. The observed frequency shift and its magnitude for one of the Fe-H bands of **3** are comparable to that observed for the Fe-(H/D)-Si moiety of (η^5-C$_5$Me$_5$)$_2$Fe$_2$(μ-
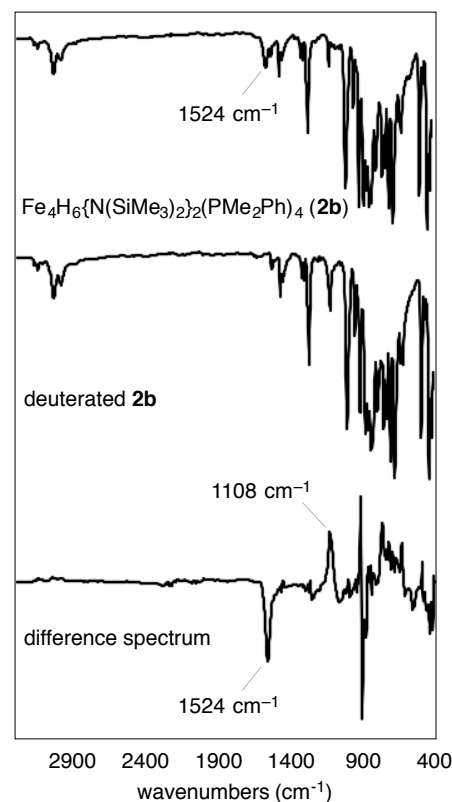

Figure 1. IR spectra of **2b** and deuterated **2b** (obtained in the presence of DBpin in toluene), as well as the corresponding difference spctrum.

H)$_2$(μ-η^2:η^2-H$_2$Si^{t}Bu$_2$) at 1736 cm^{-1} (Fe-H-Si), which shifts to 1261 cm^{-1} (Fe-D-Si).[32] The IR spectra of **2a**, **2c**, **4**, and **5** also exhibited Fe-H bands at 1508, 1548, 1566, and 1486 cm^{-1}, respectively.

In order to gain insight into the electronic properties of the Fe centers in **2b**, **3**, **4**, and **5**, ^{57}Fe Mössbauer spectra were measured on crystalline samples at zero-field and 78 K. The spectra are shown in Figure 2 and the Mössbauer parameters are listed in Table 3. [Fe$_4$] cluster **2b** exhibited two doublets in a 1:1 ratio at an isomer shift (IS) of 0.178(1) mm/s with a quadrupole splitting (QS) of 1.189(2) mm/s, and at IS = 0.592(3) mm/s with QS = 1.811(6) mm/s, both of which should accordingly be Fe(II) sites. The relatively small IS value of 0.178(1) is indicative of low-spin, phosphine-supported six-coordinate Fe(II) sites, while the large IS value of 0.592(3) is indicative of a high-spin state, leading to an assignment as the amide-supported four-coordinate Fe(II) sites. Even

Table 3. Mössbauer Parameters of 2b, 3, 4, and 5.[a]

Cluster	IS (mm/s)[b]	QS (mm/s)[b]	Area (%)	Assignment
2b	0.178(1)	1.189(2)	53	Fe-PMe$_2$Ph
	0.592(3)	1.811(6)	47	Fe-N(SiMe$_3$)$_2$
3	–0.259(3)	0.391(2)	34	FeH$_6$
	0.482(1)	0.650(2)	66	Fe-PMe$_3$
4	0.480(2)	1.173(5)	22	Fe-toluene
	0.601(1)	0.828(2)	78	Fe-N(SiMe$_3$)$_2$
5	0.153(2)	0.855(4)	50	Fe-PMe$_3$
	0.621(3)	1.276(5)	50	Fe-SDmp

[a] Measured at zero-field and 78 K with crystalline samples.

[b] IS = isomer shift (with respect to metallic iron at room temperature), QS = quadrupole splitting.

though the latter absorption was broad at 78 K (full line-width at half maximum (LW) = 0.569(9) mm/s), it sharpened at higher temperatures (Figure S22). At 200 K, the LWs of the two absorptions were comparable (0.342(13) vs. 0.277(8) mm/s), and at 250 K, the LWs were identical (0.300 mm/s). This observation may tentatively be rationalized in terms of structural fluxionality in the solid state around the amide-supported Fe site, caused $e.g.$ by a slight rearrangement of N or Fe atoms, or hydrides. It is possible that the rate of rearrangement exceeds the timescale of the Mössbauer measurement (100 ns) at higher temperatures, which would result in an averaged, relatively sharp absorption, due to motional narrowing. An analogous phenomenon was observed for thiolate-supported cluster **5**. At 78 K, the doublet assigned to the Fe-SDmp moiety (IS = 0.621(3) and QS = 1.276(5) mm/s) was slightly broader (LW = 0.345(8) mm/s) than that of the phosphine-supported Fe site (LW = 0.290(6) mm/s), while the LWs became almost identical at 150 K (0.312(9) and 0.302(7) mm/s, Figure S23). The spectrum of $[Fe_6]$ cluster **3** showed two doublets in a 1:2 ratio at IS = –0.259(3) with QS = 0.391(2) mm/s, and at IS = 0.482(1) with QS = 0.650(2) mm/s. The smaller doublet at IS = –0.259(3) mm/s was assigned to the FeH_6 sites, based on its spectral
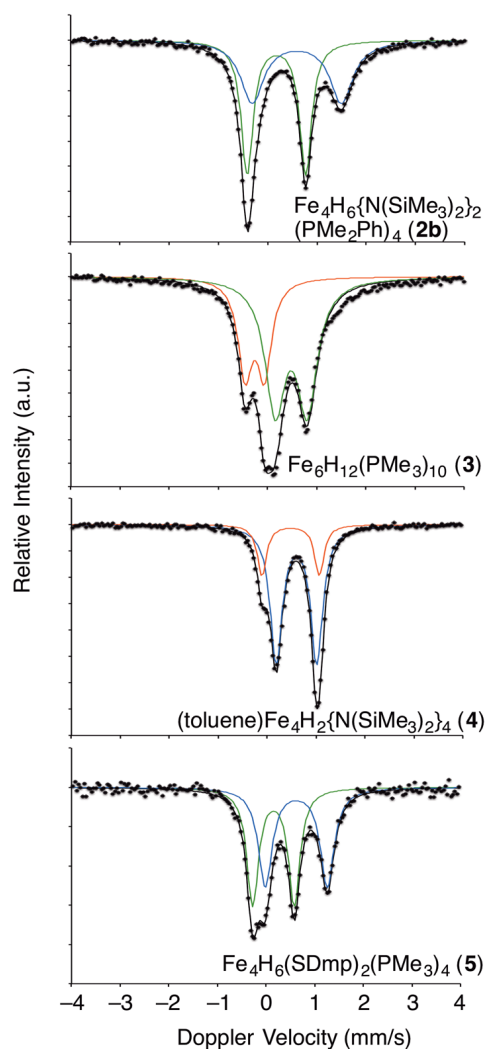
similarity to the low-spin Fe(II) compound $[Mg]_2[FeH_6]$,[33] which reveals a singlet line at IS = 0.02(1) mm/s at room temperature. The small QS value observed for the smaller doublet of **3** is also consistent with the relatively symmetric ligand arrangement of the FeH_6 sites. The larger doublet of **3** should represent the overlapped absorption of two kinds of phosphine-supported central/peripheral iron sites. Although the IS values of the two doublets differ, both still fall in the range of six- coordinate Fe(II) complexes,[34,35] while the smaller IS of –0.259(3) mm/s is close to the lower limit of low-spin and hexa-coordinate Fe(II).[35] Even though the assignment of the smaller doublet as the higher oxidation state in $e.g.$ Fe(IV) (IS = $ca.$ –0.3-+0.3)[34] should be a possibility, we are not convinced. Considering two Fe(IV) centers, the chemical formula of **3** suggests the oxidation state $Fe(IV)_2Fe(I)_4$, but the distance between the hydride-supported Fe(IV) sites and the Fe(I) sites carrying PMe_3 and hydrides are only ~2.57 Å. The oxidation states of the Fe sites should thus be more averaged, and accordingly, we tentatively assigned an all-Fe(II) oxidation state to **3**. The spectrum of toluene-supported $[Fe_4]$ cluster **4** exhibited two doublets in a 1:3 ratio at IS = 0.480(2) with QS = 1.173(5) mm/s, and at IS = 0.601(1) with QS = 0.828(2) mm/s. The smaller doublet should be assigned to the (η^6-C_7H_8)Fe site, while the larger doublet represents an averaged absorption for three amide-supported Fe centers. The IS value of the larger doublet (0.601(1) mm/s) falls within the range of typical high-spin Fe(II) complexes,[34,35] and is comparable to that assigned to the Fe(II)-N(SiMe$_3$)$_2$ sites in **2b** (0.592(3) mm/s). Considering the average Fe(+1.5) oxidation state of **4**, this result leads to a tentative $Fe(0)_1Fe(II)_3$ state, where Fe(0) resides at the (η^6-C_7H_8)Fe site. The IS and QS values of the (η^6-C_7H_8)Fe site in **4** are analogous to those of a η^6-benzene Fe(0) complex stabilized by a bis-N-heterocyclic carbene (IS = 0.43 with QS = 1.37 mm/s at 80 K),[36] the coordination geometry of which is similar to the (η^6-C_7H_8)Fe site of **4**. A tentative assignment of the $Fe(0)_1Fe(II)_3$ state should be applicable to **4**, even though the close proximity of the Fe(0) and Fe(II) centers is within the range of direct Fe-Fe interactions, which should lead to a more averaged oxidation state of the Fe atoms. Indeed, the IS value for the (η^6-C_7H_8)Fe site [0.480(2) mm/s] is slightly beyond the range of five-coordinate Fe(0) complexes (IS = 0.17-0.43 mm/s).[36]

Catalytic silylation of N_2 and attempted synthesis of NH_3 mediated by the $[Fe_4]$ and $[Fe_6]$ clusters. The phosphine-supported $[Fe_4]$ and $[Fe_6]$ hydride clusters were used for the catalytic conversion of N_2 into $N(SiMe_3)_3$, as previous reports have shown success for Fe,[37,38] Co,[39,40] Mo,[41-44] and V[45] complexes. Representative results are summarized in Table 4, while some additional results are listed in Table S1. In a typical reaction, Na and Me_3SiCl (600 equiv. each per Fe atom) were mixed with **2a-c**, **3**, **4**, or **5** in 1,2-dimethoxyethane (DME), and the mixtures were stirred at room temperature for 100 h. After addition of cyclododecane as an internal standard, the resulting reaction mixtures were analyzed by GC/GC-MS to identify and quantify the products.

$[Fe_6]$ cluster **3** was employed to screen the reaction conditions. When the reaction was conducted in DME for 100 h, 183 equiv. of $N(SiMe_3)_3$ were obtained per equiv. of **3** (31 equiv./Fe atom) (entry 4). The yields per Fe atom were higher when $[Fe_4]$ clusters were used as the catalyst precursors. For example, 159 equiv. were obtained per equiv. of **2b** (40 equiv./Fe atom), 160 equiv. per equiv. of **2c** (40 equiv./Fe atom), and 148 equiv. per equiv. of **4** (37 equiv./Fe atom) (entries 2, 3, and 8). These yields are even higher than the 34 equiv. of $N(SiMe_3)_3$ per Fe atom obtained from using

Figure 2. ^{57}Fe Mössbauer Spectra of Fe-hydride Clusters at 78 K. Blue line = Fe-N(SiMe$_3$)$_2$ or Fe-thiolate, green line = Fe-phosphine, red line = other Fe sites. The Doppler velocity scale was calibrated using room-temperature Mössbauer spectra of a metallic iron foil.

$$N_2 + 6\ Na + 6\ Me_3SiCl \xrightarrow[\substack{\text{solvent, r.t.}\\ 100\ h}]{\substack{\text{Fe-cluster}\\ (0.01\ \text{mmol})}} 2\ N(SiMe_3)_3$$
$$\text{(1 atm)} \quad \text{(600 eq. / Fe atom)}$$

Entry	Cluster	Solvent[b]	$N(SiMe_3)_3$ (eq. / cluster)	$N(SiMe_3)_3$ (eq. / Fe atom)
1	**2a**	DME	125 ± 4	31 ± 1
2	**2b**	DME	159 ± 18	40 ± 5
3	**2c**	DME	160 ± 13	40 ± 3
4	**3**	DME	183 ± 18	31 ± 3
5	**3**	THF	80 ± 23	13 ± 4
6[c]	**3**	DME	32 (KC_8)	5 (KC_8)
7[d]	**3**	DME	123 (48 h)	21 (48 h)
8	**4**	DME	148 ± 22	37 ± 6
9	**5**	DME	104 ± 5	26 ± 1

[a] r.t. = room temperature, eq. = equivalent. Yields for entries 1-5 and 8-9 are averages of three runs. Yields for entries 6-7 are averages of two runs.

[b] DME = 1,2-dimethoxyethane, THF = tetrahydrofuran, volume = 24 mL.

[c] KC_8 was used as the reductant instead of Na.

[d] Reaction time was 48 h.

$\{\eta^5\text{-}C_5H_2(SiMe_3)_3\}_2Fe$ as the catalyst precursor.[37] While THF was used as the solvent in previous studies, the present reactions afforded relatively low $N(SiMe_3)_3$ yields in THF, e.g. 80 equiv. per **3** (entry 5) and 70 equiv. per **2b**. As reported for some reactions in THF, side products such as $Me_3Si\text{-}SiMe_3$ and mono- and bis-silylated derivatives of ring-opened THF, i.e., $Me_3SiO(CH_2)_4R$ (R = H, $SiMe_3$), were found in addition to $N(SiMe_3)_3$. The product profiles as a function of the reaction time (Figure S25) revealed that silylation of the solvent was suppressed by the use of DME, where the $\cdot SiMe_3$ radicals generated from the reaction between Me_3SiCl and Na were used predominantly for the formation of $Me_3Si\text{-}SiMe_3$ and $N(SiMe_3)_3$. The higher yield of $Me_3Si\text{-}SiMe_3$ relative to that of $N(SiMe_3)_3$ in DME and THF indicates that the silylation of N_2 is slow in comparison to the dimerization of $\cdot SiMe_3$ and the side reactions of $\cdot SiMe_3$ with solvents. The lower solubility of Na in DME relative to that in THF should at least in part contribute to the long reaction time (~100 h) required in the present catalytic system. The choice of reducing agent can also affect the yield of $N(SiMe_3)_3$. For example, the use of KC_8 instead of Na afforded merely 32 and 39 equivalents of $N(SiMe_3)_3$ per **3** (entry 6) and **2b**, respectively. Lithium was not tested in this study, as the formation of lithium nitride from the reaction between lithium and pressurized N_2 occurs at high temperature in the absence of a catalyst.

Based on previous reports on the success of Fe complexes,[38,46-49] we also attempted to synthesize NH_3 from N_2. In a representative reaction, the corresponding Fe cluster was dissolved in Et_2O and cooled to –100 °C, before an excess of $HBAr^F_4\cdot 2Et_2O$ ($Ar^F = 3,5\text{-}(CF_3)_2C_6H_3$)[50] and KC_8[51] was added under an atmosphere of N_2. The yields of NH_3 and N_2H_4 were determined based on the colorization reactions,[52-54] and the results are summarized in Table S3. $[Fe_4]$ clusters **2a-c** furnished 1.31-2.41 equiv. of NH_3 per equiv. of cluster (~0.6 equiv./Fe), while the yields of N_2H_4 were virtually negligible (0.001-0.20 equiv./cluster; ~0.05 equiv./Fe atom). Us-

ing $[Fe_6]$ cluster **3**, the yield of NH_3 was even lower (0.94 equiv., 0.16 equiv./Fe). The $[Fe_4]$ clusters **2a-c** contain $-N(SiMe_3)_2$ ligands, which can be converted into NH_3 during the reactions or workup. To examine this possibility, we used **2a** to carry out a reaction under an atmosphere of $^{15}N_2$; the vacuum-transferred NH_3 after protonation with HCl exhibited ^1H NMR signals of $[^{15}NH_4][Cl]$ and $[^{14}NH_4][Cl]$ in a 77:23 ratio (Figure S29). By applying this ratio, the amount of NH_3 originating from the gas-phase N_2 can be calculated as 1.83 equiv. per equiv. of **2a**. Time-course plots of the yield of NH_3 in the reactions mediated by **2b** and **3** at –100 °C (Figure S30) revealed that the reaction with **2b** was finished after ~5 min, indicating that **2b** quickly degrades in the presence of excess $HBAr^F_4\cdot 2Et_2O$ and KC_8. Conversely, the reaction with **3** slowly occurred over the course of ~60 min, indicating that the generation of the reactive species from **3** is the rate-determining step. Extension of the reaction time (~3 h) did not improve the yield of NH_3, possibly due to the consumption of the added $HBAr^F_4\cdot 2Et_2O$ and KC_8 prior to complete conversion of **3** into the reactive species.

Possible reactive species generated from the Fe clusters. Mechanistic questions remain as to how the Fe clusters generate the catalytically active species. Although the ESI-MS spectra of the silylation reaction mixtures did not exhibit any signals associated with Fe clusters, a new ESI-MS signal that was assigned to $[Fe_6H_{10}(PMe_3)_8]^+$ ($m/z = 953.9$) was observed when an Et_2O solution of **3** was treated with $HBAr^F_4\cdot 2Et_2O$ and KC_8 (3 equiv. each) and an aliquot of the resulting solution was diluted with THF and quickly analyzed by ESI-MS (Figure 3). The presence of ten hydrides in this cluster was supported by the signal of the corresponding deuterium-labeled sample ($m/z = 963.9$) (Figure 3b). Figure 3c shows the proposed structure for $[Fe_6H_{10}(PMe_3)_8]$, in which the central Fe atoms could be stabilized by solvent molecules that are liberated under reduced pressure in the spectrometer. Even though the detection of $[Fe_6H_{10}(PMe_3)_8]$ does not confirm its presence as an intermediate in the reaction, the removal of two PMe_3 ligands and two hydrides from **3** is consistent with the results of the reaction of $[Fe_4]$ cluster **2c** with H_2SiPh_2 (Scheme 3), wherein two PEt_3 ligands and two hydrides were replaced with two molecules of H_2SiPh_2.

The reactivity of the $[Fe_4]$ and $[Fe_6]$ clusters in the absence of protons, chlorosilanes, and reductants was examined to gain insight into the behavior of these clusters toward external substrates. However, reaction products could not be identified for reactions of the clusters under an atmosphere of N_2 (1 atm, heating or UV irradiation) or CO (1 atm), or in the presence of an excess of tert-butyl isocyanide (CN^tBu). Conversely, the reaction of **2c** with excess H_2SiPh_2 furnished crystals of $Fe_4(\mu\text{-}H)_4\{N(SiMe_3)_2\}_2(PEt_3)_2(\mu\text{-}\eta^2:\eta^2\text{-}H_2SiPh_2)_2$ (**6**) (Scheme 3). Unfortunately, a detailed characterization of these crystals was hampered by the inevitable minor contaminations with paramagnetic species. As shown in Scheme 3 (bottom), two H_2SiPh_2 ligands in **6** coordinate to the central Fe atoms instead of the two μ_3-hydrides and two PEt_3 ligands in **2c**, indicating that the reaction site is located at the central Fe atoms. The assigned $\eta^2:\eta^2$-coordination mode for H_2SiPh_2 in **6** is supported by the IR spectrum and the molecular structure. The IR spectrum exhibited two broad bands at 1767 and 1561 cm^{-1}, which were assigned to the Fe-H-Si and Fe-H-Fe bands of **6**, respectively. Nevertheless, bands of minor contaminations may also appear. The Fe-Si distances determined by X-ray crystallography (2.2867(7)-2.3232(7) Å) are slightly longer than the single bonds in Fe-(μ-
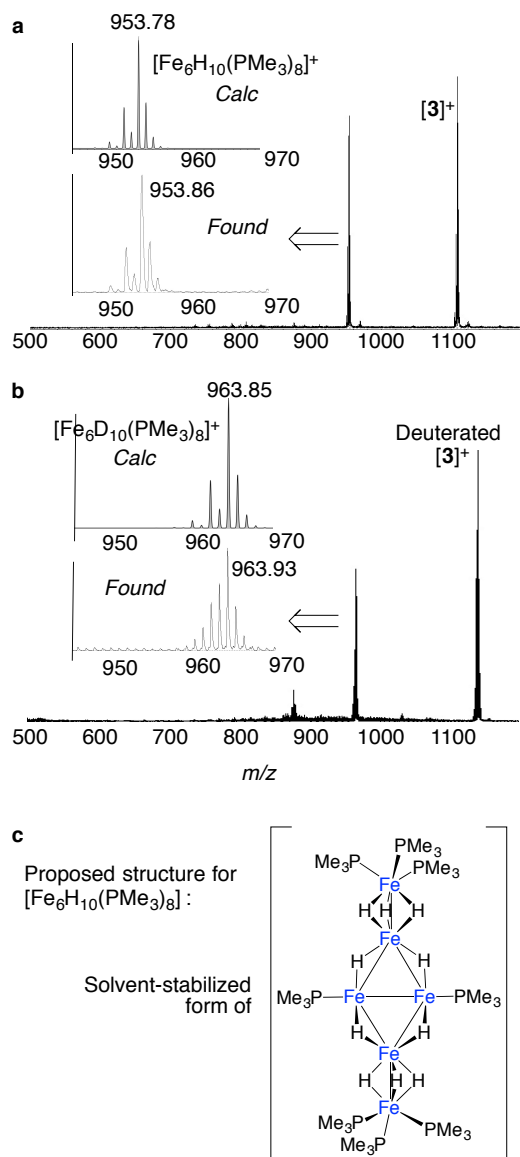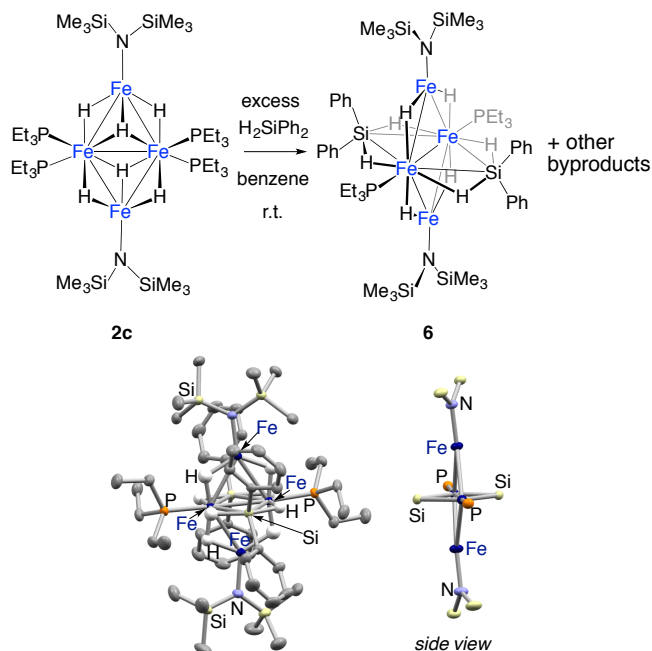
a

953.78

$[Fe_6H_{10}(PMe_3)_8]^+$
Calc

$[3]^+$

950   960   970

953.86

Found ⟵

950   960   970

500   600   700   800   900   1000   1100

b

963.85

$[Fe_6D_{10}(PMe_3)_8]^+$
Calc

Deuterated
$[3]^+$

950   960   970

963.93

Found ⟵

950   960   970

500   600   700   800   900   1000   1100

m/z

c

Proposed structure for
$[Fe_6H_{10}(PMe_3)_8]$:

Solvent-stabilized
form of

Figure 3. ESI-MS spectra obtained from treatment of the $[Fe_6]$ cluster with HBAr$^F_4$·2Et$_2$O and KC$_8$ at −100 °C. (a) Cluster **3**. (b) Deuterated **3**. (c) Proposed structure of the observed species, based on the structure of cluster **6** (Scheme 3).

SiR$_2$)-Fe complexes (2.242(3)-2.272(1) Å) and comparable to those typically reported for Fe$_2$(μ-η^2:η^2-H$_2$SiR$_2$) interactions (2.308(4)-2.3830(12) Å).[55,56] The diagonal Fe-Fe bond supported by the H$_2$SiPh$_2$ ligands (2.7591(5) Å) is slightly longer than the others (2.6695(5)-2.7416(5) Å), possibly in order to facilitate sufficient interactions between the Fe atoms and the H-Si moieties.

The aforementioned results indicate that the reaction sites should be generated at the central Fe atoms of the $[Fe_4]$ and $[Fe_6]$ clusters via dissociation of two phosphines and two hydrides. Even though the N$_2$-ligated derivatives of the Fe clusters have not yet been isolated or identified, the conversion of N$_2$ should proceed via consecutive binding of N$_2$ to the central Fe atoms, followed by sequential silylations with ·SiMe$_3$ or protonation/reduction. Previously reported theoretical analyses for the catalytic silylation of N$_2$ have suggested that silylated nitrogen species may possibly dissociate from the metal centers either as N(SiMe$_3$)$_3$ or $[N_2(SiMe_3)_3]^-$

Scheme 3. Reaction of 2c with H$_2$SiPh$_2$ and Molecular Structure of 6.[a]

2c   **6**

side view

[a] In the molecular structure (atomic displacement parameters set at 50% probability), only selected atoms are labeled, and hydrogen atoms except for the hydrides are omitted for clarity. In the side view, carbon and hydrogen atoms are omitted for clarity.

,[37,39,42] whereby the latter has been proposed to spontaneously convert into N(SiMe$_3$)$_3$ in the presence of ·SiMe$_3$ and Me$_3$SiCl.[42]

With regard to the generation of catalytically active species, one can alternatively propose fragmentation or aggregation of the Fe clusters. A tentative fragmentation of PMe$_3$-supported Fe clusters **2a** and **3** could result in the formation of FeH$_2$(PMe$_3$)$_4$ (**Fe$_1$**), $[\{(Me_3P)_3Fe\}_2(μ-H)_3]^+$ (**Fe$_2$**)[57], or their analogues. Therefore, we used **Fe$_1$** and **Fe$_2$** in the silylation reactions of N$_2$ (Table S1). However, only negligible to low amounts of N(SiMe$_3$) were obtained from the reactions of **Fe$_1$** (< 2 equiv./Fe) and **Fe$_2$** (18 equiv./Fe). Even though a tentative dissociation of Fe-N(SiMe$_3$)$_2$ moieties from $[Fe_4]$ clusters **2a-2c** may generate derivatives of Fe{N(SiMe$_3$)$_2$}$_2$ (**1**), **1** was reported to be inactive for the catalytic silylation of N$_2$.[37] Therefore, even though possibilities to split the Fe clusters in different ways still remain, we speculate here that Fe-cluster species should serve as the catalytically active species in the silylation of N$_2$. In order to examine the possibility of aggregation, silylation reactions of N$_2$ catalyzed by **3** were carried out in the presence of Hg (100 equiv.). The yields of the catalytically obtained N(SiMe$_3$) were not affected by the presence of Hg, undermining the possibility that catalytically active Fe particles are generated, although this result does not rule out the possible formation of active Fe particles due to the difficulties associated with the formation of iron-mercury amalgam.[58]

Conclusion

In summary, we synthesized a new class of $[Fe_4]$ and $[Fe_6]$ hydride clusters based on metathesis reactions between the Fe-N(SiMe$_3$)$_2$ moiety of Fe{N(SiMe$_3$)$_2$}$_2$ (**1**) and HBpin in the presence/absence of phosphines. Although the paramagnetism of these

clusters hampered a ^{1}H NMR investigation of the hydride signals, the presence of hydrides was confirmed by crystallographic and mass spectrometric analyses, as well as by the infrared spectra in combination with deuterium-labeling experiments. The phosphine-supported $[Fe_4]$ and $[Fe_6]$ hydride clusters can serve as catalyst precursors for the conversion of N_2 into $N(SiMe_3)_3$ in the presence of Na and Me_3SiCl. The catalytically active species should be generated from these clusters by dissociation of two phosphines and two hydrides. This notion is supported by the result of mass spectrometric analyses on the $[Fe_6]$ cluster and the reaction of one of the $[Fe_4]$ clusters with H_2SiPh_2.

Experimental Section

General Procedures

All reactions were carried out under an atmosphere of N_2 or Ar using either Schlenk line or glove box techniques. Hexane, toluene, THF, Et_2O, and pentane were purified by passing over columns of activated alumina and a supported copper catalyst supplied by Hansen & Co. Ltd. Benzene and DME were dried over sodium and vacuum-transferred prior to use. Deuterated solvents were dried over Na and distilled prior to use. ^{1}H NMR spectra were recorded on a JEOL JNM-ECS600 spectrometer. IR spectra were recorded on an ATR-equipped Bruker Alpha FT-IR spectrometer, while UV-vis spectra were measured on a JASCO V770 spectrometer. Elemental analyses were performed on crystalline samples sealed in tin capsules under N_2, using an Elementar Analytical vario MICRO cube elemental analyzer. Electro-spray ionization mass spectra (ESI-MS) were acquired on a JEOL JMS-T100CS spectrometer. Cyclic voltammograms were generated on a single-compartment cell under a N_2 atmosphere at room temperature using a BAS ALS-660A electrochemical analyzer. As the supporting electrolyte, 0.2 M tetrabutylammonium hexafluorophosphate ($[^nBu_4N][PF_6]$) was used, which was recrystallized from THF prior to use. Potentials are referenced to the ferrocene/ferrocenium cation (Fc/Fc^+) couple *via* measurements in the presence of ferrocene. Mössbauer measurements were performed in a conventional transmission mode on a Mössbauer spectrometer (Toporogic System Co. Model-222) with a $^{57}Co(Rh)$ source (925 MBq). The spectral curve fitting was carried out by using MossWinn 4.0Pre on the assumption of the sum of the Lorentzian curves. The Doppler velocity scale was calibrated with respect to α-iron at room temperature, and the isomer shifts are given relative to α-iron. GC/GC-MS analyses were acquired on a Shimadzu GCMS-2010SE. Low-temperature experiments were carried out in a glove box using a Techno Sigma UCR-150-GB. $Fe\{N(SiMe_3)_2\}_2$ (**1**)[19], HSDmp[27], HBAr$^F_4$·2Et$_2$O[50], and KC$_8$[51] were prepared according to previously reported procedures. All other chemicals were purchased from common commercial sources and used without further purification. Deuterated cluster samples were prepared by using deuterated pinacolborane (DBpin)[59] instead of HBpin.

Fe$_4$(μ-H)$_4$(μ$_3$-H)$_2$\{N(SiMe$_3$)$_2$\}$_2$(PMe$_3$)$_4$ (2a). A toluene solution of PMe$_3$ (1 M, 2.66 mL, 2.66 mmol) was added to **1** (1.00 g, 2.66 mmol) at room temperature. The resulting colorless solution was cooled to –30 °C and HBpin (0.58 mL, 4.00 mmol) was added dropwise. The color of the reaction mixture quickly turned to black. After stirring for 1 h at –30 °C, the mixture was kept standing overnight at room temperature, before being stored in a freezer at –30 °C, which furnished black blocks of **2a** (0.0735 g, 0.086 mmol, 13%). Crystals were collected after washing with hexane (*ca.* 3 x 5

mL) and drying under vacuum. ^{1}H NMR (600 MHz, C_6D_6, r.t.): δ 47.3 ($w_{1/2}$ = 500 Hz, Si*Me*$_3$), –75.1 ($w_{1/2}$ = 280 Hz, P*Me*$_3$). UV-vis (THF): λ_{max} = 258 (ε 6.5 x 10^3 cm^{-1}M^{-1}) nm. Solution magnetic moment (C_6D_6, 298 K): 8.7(3) μ$_B$. IR (ATR, cm^{-1}): ν = 2971, 2945, 2906, 1508, 1419, 1297, 1281, 1237, 1065, 994, 931.

Fe$_4$(μ-H)$_4$(μ$_3$-H)$_2$\{N(SiMe$_3$)$_2$\}$_2$(PMe$_2$Ph)$_4$ (2b). A toluene (2.0 mL) solution of PMe$_2$Ph (0.36 g, 2.62 mmol) was added to **1** (1.00 g, 2.66 mmol) at room temperature. The resulting mixture was cooled to –30 °C and HBpin (0.58 mL, 4.00 mmol) was added dropwise. After stirring for 1 h at –30 °C, the mixture was kept standing overnight at room temperature, before being stored in a freezer at –30 °C, which furnished black blocks of **2b** (0.078 g, 0.071 mmol, 11%). Crystals were collected after washing with hexane (*ca.* 3 x 5 mL) and drying under vacuum. ^{1}H NMR (600 MHz, C_6D_6, r.t.): δ 50.7 ($w_{1/2}$ = 550 Hz, Si*Me*$_3$), –7.1 ($w_{1/2}$ = 40 Hz, *p*-Ph), –13.1 ($w_{1/2}$ = 40 Hz, *o*- or *m*-Ph), –79.0 ($w_{1/2}$ = 650 Hz, *o*- or *m*-Ph), –84.7 ($w_{1/2}$ = 390 Hz, PC*H*$_3$). Cyclic Voltammetry (THF): $E_{1/2}$ = –0.58 V, –2.11 V (vs. Fc/Fc$^+$). UV-vis (THF): λ_{max} = 250 (ε 4.5 x 10^4 cm^{-1}M^{-1}) nm. Solution magnetic moment (C_6D_6, 298 K): 8.3(1) μ$_B$. IR (ATR, cm^{-1}): ν = 3079, 3055, 2948, 2906, 1524, 1488, 1433, 1419, 1290, 1276, 1239, 1098, 986, 932. Mössbauer spectrum (mm/s, 78 K): IS = 0.178(1) and QS = 1.189(2) (53% intensity), IS = 0.592(3) and QS = 1.811(6) (47% intensity). Anal. Calcd for $C_{44}H_{86}Si_4N_2P_4Fe_4$: C, 47.90; H, 7.86; N, 2.54. Found: C, 48.40; H, 7.40; N, 2.38.

Fe$_4$(μ-H)$_4$(μ$_3$-H)$_2$\{N(SiMe$_3$)$_2$\}$_2$(PEt$_3$)$_4$ (2c). A toluene solution of PEt$_3$ (20 wt%, 7.82 g, 13.2 mmol) was added to **1** (4.96 g, 13.2 mmol) at room temperature to give a pale yellow solution. HBpin (2.90 mL, 20.0 mmol) was added dropwise at room temperature. The color of the reaction mixture quickly turned to black. After stirring for 20 min, the mixture was filtered through a disposable filter (Whatman 25 mm) to remove a small amount of black solid. The solution was kept at room temperature overnight, before being stored in a freezer at –30 °C, which furnished black blocks of **2c** (0.62 g, 0.606 mmol, 18%). Crystals were collected after washing with hexane (*ca.* 5 x 10 mL) and drying under vacuum. ^{1}H NMR (600 MHz, C_6D_6, r.t.): δ 49.8 ($w_{1/2}$ = 520 Hz, Si*Me*$_3$), –57.7 ($w_{1/2}$ = 270 Hz, P(CH$_2$C*H*$_3$)$_3$), –84.6 ($w_{1/2}$ = 390 Hz, P(C*H*$_2$CH$_3$)$_3$). UV-vis (THF): λ_{max} = 262 (ε 1.5 x 10^4 cm^{-1}M^{-1}) nm. Solution magnetic moment (C_6D_6, 298 K): 11.2(1) μ$_B$. IR (ATR, cm^{-1}): ν = 2959, 2935, 2906, 2879, 1548, 1452, 1426, 1378, 1240, 1030, 976.

Fe$_6$(μ-H)$_{10}$(μ$_3$-H)$_2$(PMe$_3$)$_{10}$ (3). A toluene solution of PMe$_3$ (1 M, 8.0 mL, 8.0 mmol) was added to **1** (3.00 g, 7.98 mmol) at room temperature. The resultant mixture was cooled to 0 °C and HBpin (1.71 mL, 12.0 mmol) was added dropwise. The color of the reaction mixture quickly turned to black. After stirring for 60 min at 0 °C, a mixture containing a toluene solution of PMe$_3$ (1 M, 12.0 mL, 12.0 mmol) and **1** (1.50 g, 3.99 mmol) was added, before HBpin (1.71 mL, 12.0 mmol) was added. The mixture was stirred for 30 min before being kept standing for 3 days at room temperature, which furnished black blocks of **3** (0.21 g, 0.190 mmol, 14%). Crystals were collected after washing with hexane (*ca.* 3 x 5 mL) and drying under vacuum. ^{1}H NMR (600 MHz, C_6D_6, r.t.): δ 42.0 ($w_{1/2}$ = 350 Hz, P*Me*$_3$ x 6), –71.5 ($w_{1/2}$ = 310 Hz, P*Me*$_3$ x 4). Cyclic Voltammetry (THF): $E_{1/2}$ = –1.76 V, –2.96 V (vs. Fc/Fc$^+$). UV-vis (THF): λ_{max} = 250 (ε 5.5 x 10^4 cm^{-1}M^{-1}) nm. Solution magnetic moment (C_6D_6, 298 K): 6.8(3) μ$_B$. IR (ATR, cm^{-1}): ν = 2960, 2896, 2798, 1670, 1610, 1498, 1420, 1291, 1268, 1122, 920. Mössbauer

spectrum (mm/s, 78 K): IS = –0.259(3) and QS = 0.391(2) (34% intensity), IS = 0.482(1) and QS = 0.650(2) (66% intensity). ESI-MS (THF): m/z = 1108.0 ([3]$^+$).

(η^6-C$_7$H$_8$)Fe$_4$(μ-H)$_2${μ-N(SiMe$_3$)$_2$}$_2${N(SiMe$_3$)$_2$}$_2$ (4). A toluene (1.0 mL) solution of **1** (1.00 g, 2.66 mmol) was cooled at 0 °C, before HBpin (0.39 mL, 2.66 mmol) was added dropwise. After stirring for 1 h, the mixture was stored at –30 °C, which furnished a black solid. This solid was washed with pre-cooled (–30 °C) hexane (*ca.* 5 mL x 2) to leave black crystals of **4** (76.4 mg, 0.080 mmol, 12%). ^{1}H NMR (600 MHz, C$_6$D$_6$, r.t.): δ 53.4 ($w_{1/2}$ = 1000 Hz, *o*- or *m*-C$_6$H$_5$CH$_3$), –1.9 ($w_{1/2}$ = 170 Hz, Si*Me$_3$*), –5.3 ($w_{1/2}$ = 190 Hz, Si*Me$_3$*), –12.5 ($w_{1/2}$ = 180 Hz, *p*-C$_6$H$_5$CH$_3$), –20.7 ($w_{1/2}$ = 100 Hz, C$_6$H$_5$C*H$_3$*), –23.6 ($w_{1/2}$ = 550 Hz, *o*- or *m*-C$_6$H$_5$CH$_3$). Cyclic Voltammetry (THF): E_{pc} = –2.20 V (vs. Fc/Fc$^+$). UV-vis (THF): λ_{max} = 262 (ϵ 3.9 x 10^3 cm^{-1}M^{-1}) nm. Solution magnetic moment (C$_6$D$_6$, 298 K): 5.7(1) μ_B. IR (ATR, cm^{-1}): ν = 2952, 2904, 1566, 1243, 935. Mössbauer spectrum (mm/s, 78 K): IS = 0.480(2) and QS = 1.173(5) (22% intensity), IS = 0.601(1) and QS = 0.828(2) (78% intensity). Anal. Calcd for C$_{31}$H$_{82}$Si$_8$N$_4$Fe$_4$: C, 38.82; H, 8.62; N, 5.84. Found: C, 38.52; H, 8.29; N, 5.77.

Fe$_4$(μ-H)$_4$(μ_3-H)$_2$(SDmp)$_2$(PMe$_3$)$_4$ (5, Dmp = 2,6-(mesityl)$_2$C$_6$H$_3$). In a similar manner to the synthesis of **2a**, a toluene solution of PMe$_3$ (1 M, 2.66 mL, 2.66 mmol) was added to **1** (1.00 g, 2.66 mmol), before HBpin (0.58 mL, 4.00 mmol) was added dropwise at –30 °C. After stirring for 1 h to generate **2a**, the mixture was gradually warmed to room temperature. A toluene (8 mL) solution of HSDmp (461 mg, 1.33 mmol) was added at room temperature, before stirring was continued for 1 day. The solvent was evaporated to dryness, and the residue was dissolved in the minimal amount of toluene (*ca.* 10 mL). The toluene solution was transferred to a glass tube, and hexane (*ca.* 70 mL) was carefully layered on top of the black solution. Slow diffusion between two layers over a week at room temperature led to the formation of black blocks of **5** (91.1 mg, 0.074 mmol, 11%). Crystals were collected after washing with hexane (*ca.* 3 x 5 mL) and drying under vacuum. ^{1}H NMR (600 MHz, C$_6$D$_6$, r.t.): δ 68.2 ($w_{1/2}$ = 200 Hz, *m*-mesityl), 28.8 ($w_{1/2}$ = 380 Hz, *o*-mesityl), 7.07 (Ar-*H*), 6.87 (Ar-*H*), 6.66 (Ar-*H*), 2.20 (mesityl-C*H$_3$*), 2.13 (mesityl-C*H$_3$*), –5.4 ($w_{1/2}$ = 680 Hz, *p*-mesityl), –37.8 ($w_{1/2}$ = 220 Hz, P*Me$_3$*). Cyclic Voltammetry (THF): $E_{1/2}$ = –1.07 V, –2.54 V (vs. Fc/Fc$^+$). UV-vis (THF): λ_{max} = 270 (sh, ϵ 1.4 x 10^4 cm^{-1}M^{-1}) nm. Solution magnetic moment (C$_6$D$_6$, 298 K): 10.4(3) μ_B. IR (ATR, cm^{-1}): ν = 2956, 2904, 2855, 1611, 1579, 1486, 1453, 1439, 1416, 1387, 1373, 1295, 1274, 1047, 935. Mössbauer spectrum (mm/s, 78 K): IS = 0.153(2) and QS = 0.855(4) (50% intensity), IS = 0.621(3) and QS = 1.276(5) (50% intensity). ESI-MS (THF): m/z = 1224.4 ([5]$^+$). Anal. Calcd for C$_{60}$H$_{92}$P$_4$S$_2$Fe$_4$: C, 58.84; H, 7.57; S, 5.24. Found: C, 59.01; H, 7.39; S, 5.63.

Formation of a precipitate containing crystals of Fe$_4$(μ-H)$_4${N(SiMe$_3$)$_2$}$_2$(PEt$_3$)$_2$(μ-η^2:η^2-H$_2$SiPh$_2$) (6). Cluster **2c** (302 mg, 0.30 mmol) was dissolved in benzene (25 mL), and H$_2$SiPh$_2$ (1.0 mL, 5.39 mmol) was added. After stirring for 3 h at room temperature, the solvent was removed under reduced pressure. The residue was extracted with a mixture of THF and hexane (v/v = 1:3, 10 mL), and the solution was stored at –30 °C, which furnished a crystalline precipitate (64.2 mg) containing black blocks of **6**, which was washed with hexane (*ca.* 10 mL) and dried *in vacuo*. The presence of minor paramagnetic impurities was evident from the ^{1}H NMR spectrum. ^{1}H NMR (600 MHz, C$_6$D$_6$, r.t.): signals assign-able to **6** appeared at δ 43.9 ($w_{1/2}$ = 540 Hz, Si*Me$_3$*), –11.3 ($w_{1/2}$ = 80 Hz, *p-Ph*), –15.5 ($w_{1/2}$ = 170 Hz, *o*- or *m-Ph*), –25.2 ($w_{1/2}$ = 770 Hz, *o*- or *m-Ph*), –39.9 ($w_{1/2}$ = 130 Hz, P(CH$_2$CH$_3$)$_3$), –65.4 ($w_{1/2}$ = 270 Hz, P(C*H$_2$*CH$_3$)$_3$). IR (ATR, cm^{-1}): bands assignable to **6** appeared at 1767 (Fe-H-Si) and 1561 (Fe-H-Fe) cm^{-1}.

Formation of trace amounts of crystals containing both Fe$_7$(μ_3-H)$_6${μ-N(SiMe$_3$)$_2$}$_6$ and Fe$_6$(μ_3-H)$_4$(μ-H)$_2${μ-N(SiMe$_3$)$_2$}$_4${N(SiMe$_3$)$_2$}$_2$. At room temperature, HBpin (96 μL, 0.85 mmol) was added dropwise to a hexane (8 mL) solution of **1** (250 mg, 0.66 mmol). The color of the reaction mixture quickly turned to red and then to black. After stirring for 1 h, the mixture was centrifuged to remove a small amount of a black solid. The solution was concentrated to *ca.* 2 mL under reduced pressure, before being stored at –30 °C, which afforded a small amount of black crystals containing both Fe$_7$(μ_3-H)$_6${μ-N(SiMe$_3$)$_2$}$_6$ and Fe$_6$(μ_3-H)$_4$(μ-H)$_2${μ-N(SiMe$_3$)$_2$}$_4${N(SiMe$_3$)$_2$}$_2$ as the minor and major components, respectively. This mixture was characterized only by single-crystal X-ray diffraction analysis.

Unsuccessful elemental analyses for some Fe-hydride clusters. We have been unable to obtain satisfactory elemental analysis values for clusters **2a**, **2c**, and **3**. Even though a number of attempts have been made, single crystals of diffraction quality afforded low carbon and hydrogen values, possibly due to the dissociation of H$_2$ and phosphines from these molecules. Other possibilities include incomplete combustion or different ways of thermal degradation, although we cannot rule out the possibility of contamination definitively. The addition of a combustion accelerator (WO$_3$ powder) did not improve the results. The range of results observed for cluster samples and the calculated ratio of elements are as follows: (**2a**) Anal. Calcd for C$_{24}$H$_{78}$Si$_4$N$_2$P$_4$Fe$_4$: C, 33.70; H, 9.20; N, 3.28. Found: C, 31.98~32.44; H, 8.56~8.58; N, 3.36~3.42. (**2c**) Anal. Calcd for C$_{36}$H$_{102}$Si$_4$N$_2$P$_4$Fe$_4$: C, 42.27; H, 10.05; N, 2.74. Found: C, 38.27~41.04; H, 8.34~9.52; N, 2.56~2.87. (**3**) Anal. Calcd for C$_{30}$H$_{102}$P$_6$Fe$_6$: C, 32.52; H, 9.28. Found: C, 30.45~32.14; H, 7.94~8.42.

A typical procedure for the catalytic synthesis of silylamine in the presence of Fe-hydride clusters. The following procedure is analogous to those in references 37-38. A 100 mL round-bottom flask was charged with Na (0.826 g, 36 mmol) and DME (15 mL) to furnish a suspension. Cluster **3** (11.1 mg, 0.01 mmol) weighed into a glass tube and Me$_3$SiCl (4.53 mL, 36 mmol) were added sequentially. Any remaining **3** in the glass tube was dissolved in DME (9 mL) and added subsequently. The flask was attached to a balloon containing N$_2$ (1 atm), and the mixture was stirred at room temperature for 100 h. Cyclododecane (0.060 g, 0.36 mmol) was added as an internal standard for the GC analysis. After stirring for 5 min, the mixture was centrifuged, and the supernatant was subjected to GC/GC-MS.

Typical procedure for the attempted synthesis of NH$_3$ in the presence of Fe-hydride clusters. The following procedure is analogous to those reported in references 46-49. In a glove box filled with N$_2$, **3** (2.0 mg, 1.8 μmol) was dissolved in Et$_2$O in one arm of an H-shaped reaction vessel (see Figure S27). This solution was cooled to –100 °C with a cooling device (UCR-150-GB). HBAr$^F_4$·2Et$_2$O (78 mg, 77 mmol) and KC$_8$ (12 mg, 92 mmol) were added sequentially, before the walls were rinsed with Et$_2$O and the glassware sealed (total volume of Et$_2$O = 2.0 mL). This mixture was stirred for 60 min at –100 °C, before being warmed to room temperature. All volatile materials were vacuum-transferred to the

other arm of the H-shaped vessel. The residual solid was treated with a THF solution of sodium *tert*-butoxide (1.0 mL, 40 mg/mL), and the mixture was stirred for 10 min to convert NH_4 salts into NH_3. Volatiles from this mixture were combined with the other, previously collected volatiles in the other arm of the vessel via vacuum-transfer, and an Et_2O solution of HCl (2 M, 3.0 mL, 6.0 mmol) was added to the combined frozen volatiles. The glassware was warmed to room temperature and stirred for 15 min. Volatile materials were removed under reduced pressure to afford a colorless solid containing salts of NH_4 and N_2H_5. This solid was dissolved in H_2O (10 mL) in a volumetric flask. An aliquot (2.5 mL) of this solution was analyzed by color reactions.[52-54] For analyses of NH_3 and N_2H_4, calibration curves were recorded periodically. The quantification of H_2 was not carried out, because the NH_3/N_2H_4 yields remained sub-stoichiometric with respect to the Fe atoms.

X-ray Crystallographic Structure Determinations. Crystal data and refinement parameters for **2a-c**, **3-6**, and $Fe_7(\mu_3\text{-}H)_6\{\mu\text{-}N(SiMe_3)_2\}_6$ (40%)/$Fe_6(\mu_3\text{-}H)_4(\mu\text{-}H)_2\{\mu\text{-}N(SiMe_3)_2\}_4\{N(SiMe_3)_2\}_2$ (60%) are summarized in Table S4. Single crystals were coated with oil (Immersion Oil, type B: Code 1248, Cargille Laboratories, Inc.) and mounted on loops. Diffraction data were collected at –100 °C under a cold N_2 stream on a Rigaku RA-Micro7 spectrometer equipped with a Saturn70 CCD detector or a PILATUS 200K detector, using graphite-monochromated Mo Kα radiation (λ = 0.710690 Å). Six preliminary data frames were measured at 0.5° increments of ω in order to determine the crystal quality and preliminary unit cell parameters. Intensity images were also measured at 0.5° increments of ω. The frame data were integrated using the CrystalClear program package, and the data sets were corrected for absorption using the REQAB program. Calculations were performed with the CrystalStructure program package. All structures were solved by direct methods and refined by full-matrix least squares. Anisotropic refinement was applied to all non-hydrogen atoms except for disordered atoms, which were refined isotropically. All hydrogen atoms were allocated calculated positions except for the hydride ligands in **2a-c** and **3-6**, which were refined isotropically. Hydrides in $Fe_7(\mu_3\text{-}H)_6\{\mu\text{-}N(SiMe_3)_2\}_6$/$Fe_6(\mu_3\text{-}H)_4(\mu\text{-}H)_2\{\mu\text{-}N(SiMe_3)_2\}_4\{N(SiMe_3)_2\}_2$ were fixed and not refined.

ASSOCIATED CONTENT

Supporting Information

Spectroscopic data and molecular structures of the Fe-hydride clusters; additional data for catalytic reactions; a table for the crystal data and the refinement summary (pdf). The Supporting Information is available free of charge on the ACS Publications website.

AUTHOR INFORMATION

Corresponding Author

* ohki@chem.nagoya-u.ac.jp

Notes

The authors declare the absence of any competing financial interests.

ACKNOWLEDGMENT

REFERENCES

(1) Spatzal, T.; Aksoyoglu, M.; Zhang, L.; Andrade, S. L. A.; Schleicher, E.; Weber, S.; Rees, D. C.; Einsle, O. *Science* **2011**, *334*, 940.

(2) Lancaster, K. M.; Roemelt, M.; Ettenhuber, P.; Hu, Y.; Ribbe, M. W.; Neese, F.; Bergmann, U.; DeBeer, S. *Science* **2011**, *334*, 974-977.

(3) Hoffman, B. M.; Lukoyanov, D.; Yang, Z.–Y.; Dean, D. R.; Seefeldt, L. C. *Chem. Rev.* **2014**, *114*, 4041-4062.

(4) Spatzal, T.; Perez, K. A.; Einsle, O.; Howard, J. B.; Rees, D. C. *Science* **2014**, *345* ,1620-1623.

(5) Yanga, Z.–Y.; Khadkaa, N.; Lukoyanovb, D.; Hoffman, B. M.; Dean, D. R.; Seefeldt, L. C. *Proc. Natl. Acad. Sci. U.S.A.*, **2013**, *110*, 16327-16332.

(6) Lukoyanov, D.; Yang, Z.–Y.; Khadka, N.; Dean, D. R.; Seefeldt, L. C.; Hoffman, B. M. *J. Am. Chem. Soc.* **2015**, *137*, 3610-3615.

(7) Spencer, N. D.; Schoonmaker, R. C.; Somorjai, G. A. *J. Catal.* **1982**, *74*, 129-135.

(8) Ertl, G. *J. Vac. Sci. Technol., A* **1983**, *1*, 1247-1253.

(9) Mortensen, J. J.; Hansen, L. B.; Hammer, B.; Nørskov, J. K. *J. Catal.* **1999**, *182*, 479-488.

(10) Ertl, G. In *Catalytic Ammonia Synthesis: Fundamentals and Practice in Fundamental and Applied Catalysis*; Jennings J. R., Ed.; Springer: New York, **1991**.

(11) Fryzuk, M. D.; Johnson, S. A.; Patrick, B. O.; Albinati, A.; Mason, S. A.; Koetzle, T. F. *J. Am. Chem. Soc.* **2001**, *123*, 3960-3973.

(12) Akagi, F.; Matsuo, T.; Kawaguchi, H. *Angew. Chem. Int. Ed.* **2007**, *46*, 8778-8781.

(13) Shima, T.; Hu, S.; Luo, G.; Kang, X.; Luo, Y.; Hou, Z. *Science* **2013**, *340*, 1549-1552.

(14) Yu, Y.; Sadique, A. R.; Smith, J. M.; Dugan, T. R.; Cowley, R. E.; Brennessel, W. W.; Flaschenniem, C. J.; Bill, E.; Cundari, T. R.; Holland, P. L. *J. Am. Chem. Soc.* **2008**, *130*, 6624-6638.

(15) Ding, K.; Brennessel, W. W.; Holland, P. L. *J. Am. Chem. Soc.* **2009**, *131*, 10804-10805.

(16) Rittle, J.; McCrory, C. C.; Peters, J. C. *J. Am. Chem. Soc.* **2014**, *136*, 13853-13862.

(17) Ohki, Y.; Takikawa, Y.; Hatanaka, T.; Tatsumi, K. *Organometallics* **2006**, *25*, 3111-3113.

(18) Ohki, Y.; Shimizu, Y.; Araake, R.; Tada, M.; Sameera, W. M. C.; Ito, J.; Nishiyama, H. *Angew. Chem. Int. Ed.*, **2016**, *55*, 15821-15825.

(19) Andersen, R. A.; Faegri, K.; Green, J. C.; Haaland, A.; Lappert, M. F.; Leung, W.-P.; Rypdal, K. *Inorg. Chem.* **1988**, *27*, 1782–1786.

(20) The reaction of crystalline **2a** (81 mg) with **1**, PMe$_3$, and HBpin furnished crystals of **3** (5 mg, 5 %). The low crystal yield possibly due to the small reaction scale. Although a single-step reaction of **1** (533 mg) with PMe$_3$ and HBpin in the ratio of 6(Fe):10(PMe$_3$):12(HBpin) seems suitable for the synthesis of **3**, this reaction afforded merely traces of **3** (8 mg), thus corroborating the importance to generate **2a** for the successful synthesis of **3**.

(21) Gieshoff, T. N.; Chakraborty, U.; Villa, M.; Jacobi von Wangelin, A. *Angew. Chem. Int. Ed.* **2017**, doi 10.1002/anie.201612548.

(22) For the corresponding shortest Fe-P distance listed in the Cambridge Structural Database, see: Henry, R. M.; Shoemaker, R. K.; Newell, R. H.; Jacobsen, G. M.; DuBois, D. L.; DuBois M. R. *Organometallics* **2005**, *24*, 2481-2491.

(23) For the corresponding longest Fe-P distance listed in the Cambridge Structural Database, see: Kohl, S. W.; Heinemann, F. W.;

Hummert, M.; Bauer, W.; Grohmann, A. *Dalton Trans.* **2006**, 5583-5592.

(24) For the corresponding shortest Fe-N distance listed in the Cambridge Structural Database, see: Verma, A. K.; Lee, S. C. *J. Am. Chem. Soc.* **1999**, *121*, 10838-10839.

(25) For the corresponding longest Fe-N distance listed in the Cambridge Structural Database, see: Day, B. M.; Pugh, T.; Hendriks, D.; Guerra, C. F.; Evans, D. J.; Bickelhaupt, F. M.; Layfield, R. A. *J. Am. Chem. Soc.* **2013**, *135*, 13338-13341.

(26) For the corresponding shortest/longest Fe–{μ-N(SiMe$_3$)$_2$}–Fe distances listed in the Cambridge Structural Database, see reference 17 and Malassa, A.; Schulze, B.; Stein-Schaller, B.; Gorls, H.; Weber, B.; Westerhausen, M. *Eur. J. Inorg. Chem.* **2011**, 1584-1592.

(27) Ellison, J. J.; Ruhlandt-Senge, K.; Power, P. P. *Angew. Chem. Int. Ed. Engl.* **1994**, *33*, 1178-1180.

(28) Ohki, Y.; Ikagawa, Y.; Tatsumi, K. *J. Am. Chem. Soc.* **2007**, *129*, 10457-10465.

(29) Ohta, S.; Ohki, Y.; Ikagawa, Y.; Suizu, R.; Tatsumi, K. *J. Organomet. Chem.* **2007**, *692*, 4792-4799.

(30) Hashimoto, T.; Ohki, Y.; Tatsumi, K. *Inorg. Chem.* **2010**, *49*, 6102-6109.

(31) Ohta, S.; Ohki, Y.; Hashimoto, T.; Cramer, R. E.; Tatsumi, K. *Inorg. Chem.* **2012**, *51*, 11217-11219.

(32) Ohki, Y.; Kojima, T.; Oshima, M.; Suzuki, H. *Organometallics* **2001**, *20*, 2654-2656.

(33) Didisheim, J. –J.; Zolliker, P.; Yvon, K.; Fischer, P.; Schefer, J. Gubelmann, M.; Williams, A. F. *Inorg. Chem.* **1984**, *23*, 1953-1957.

(34) Gütlich, P.; Bill, E.; Trautwein, A. X. In *Mössbauer Spectroscopy and Transition Metal Chemistry, Fundamentals and Applications*; Springer: Heidelberg, **2011**, and references therein.

(35) Vandenberghe, R. E.; De Grave, E. In *Mössbauer Spectroscopy– Tutorial Book*; Yoshida, Y.; Langouche, G., Eds.; Springer: Heidelberg, **2013**, and references therein.

(36) Blom, B.; Tan, G.; Enthaler, S.; Inoue, S.; Epping, J. D.; Driess, M. *J. Am. Chem. Soc.* **2013**, *135*, 18108-18120.

(37) Yuki, M.; Tanaka, H.; Sasaki, K.; Miyake, Y.; Yoshizawa, K.; Nishibayashi, Y. *Nat. Commun.* **2012**, *3*, 1254.

(38) Ung, G.; Peters, J. C. *Angew. Chem. Int. Ed.* **2015**, *54*, 532-535.

(39) Siedschlag, R. B.; Bernales, V.; Vogiatzis, K. D.; Planas, N.; Clouston, L. J.; Bill, E.; Gagliardi, L.; Lu, C. C. *J. Am. Chem. Soc.* **2015**, *137*, 4638-4641.

(40) Imayoshi, R.; Tanaka, H.; Matsuo, Y.; Yuki, M.; Nakajima, K.; Yoshizawa, K.; Nishibayashi, Y. *Chem.–Eur. J.* **2015**, *21*, 8905-8909.

(41) Komori, K.; Oshita, H.; Mizobe, Y.; Hidai, M. *J. Am. Chem. Soc.* **1989**, *111*, 1939-1940.

(42) Tanaka, H.; Sasada, A.; Kouno, T.; Yuki, M.; Miyake, Y.; Nakanishi, H.; Nishibayashi, Y.; Yoshizawa, K. *J. Am. Chem. Soc.* **2011**, *133*, 3498-3506.

(43) Ogawa, T.; Kajita, Y.; Wasada-Tsutsui, Y.; Wasada, H.; Masuda, H. *Inorg. Chem.* **2013**, *52*, 182-195.

(44) Liao, Q.; Saffon-Merceron, N.; Mézailles, N. *Angew. Chem. Int. Ed.* **2014**, *53*, 14206-14210.

(45) Imayoshi, R.; Nakajima, K.; Nishibayashi, Y. *Chem. Lett.* **2017**, *46*, 466-468.

(46) Anderson, J. S.; Rittle, J.; Peters, J. C. *Nature* **2013**, *501*, 84-87.

(47) Creutz, S. E.; Peters, J. C. *J. Am. Chem. Soc.* **2014**, *136*, 1105-1115.

(48) Del Castillo, T. J.; Thompson, N. B.; Peters, J. C. *J. Am. Chem. Soc.* **2016**, *138*, 5341-5350.

(49) Kuriyama, S.; Arashiba, K.; Nakajima, K.; Matsuo Y.; Tanaka, H.; Ishii, K. Yoshizawa, K.; Nishibayashi, Y. *Nat. Commun.* **2016**, *7*, 12181.

(50) Brookhart, M.; Grant, B.; Volpe, A. F. Jr. *Organometallics* **1992**, *11*, 3920-3922.

(51) Bergbreiter, D. E.; Killough, J. M. *J. Am. Chem. Soc.* **1978**, *100*, 2126-2134.

(52) Chaney, A. L.; Marbach, E. P. *Clin. Chem.* **1962**, *8*, 130-132.

(53) Weatherburn, M. W. *Anal. Chem.* **1967**, *39*, 971-974.

(54) Watt, G. W.; Chrisp, J. D. *Anal. Chem.* **1952**, *24*, 2006-2008.

(55) Corey, J. Y.; Braddock-Wilking, J. *Chem. Rev.* **1999**, *99*, 175-292.

(56) Corey, J. Y. *Chem. Rev.* **2011**, *111*, 863-1071.

(57) Gusev, D. G.; Hübener, R.; Burger, P.; Orama, O.; Berke, H. *J. Am. Chem. Soc.* **1997**, *119*, 3716-3731.

(58) Linderoth, S.; Morup, S. *J. Phys. Condens. Matter* **1992**, *4*, 8627-8634.

(59) Wei, C. S.; Jiménez-Hoyos, C. A.; Videa, M. F.; Hartwig, J. F.; Hall, M. B. *J. Am. Chem. Soc.* **2010**, *132*, 3078-3091.

Authors are required to submit a graphic entry for the Table of Contents (TOC) that, in conjunction with the manuscript title, should give the reader a representative idea of one of the following: A key structure, reaction, equation, concept, or theorem, etc., that is discussed in the manuscript. Consult the journal's Instructions for Authors for TOC graphic specifications.

$$6\ Na + 6\ Me_3SiCl + N_2 \longrightarrow N(SiMe_3)_2 \quad \begin{array}{l} \sim 160\ eq./\ \mathbf{Fe_4} \\ 183\ eq./\ \mathbf{Fe_6} \end{array}$$